INTERFACE

royalsocietypublishing.org/journal/rsif

Research



Cite this article: Krishnamurthy D, Pepper R, Prakash M. 2023 Active sinking particles: sessile suspension feeders significantly alter the flow and transport to sinking aggregates.

J. R. Soc. Interface 20: 20220537.

https://doi.org/10.1098/rsif.2022.0537

Received: 25 July 2022 Accepted: 4 January 2023

Subject Category: Life Sciences-Physics interface

Subject Areas: biomechanics, biophysics

Keywords:

Vorticella, marine snow, lake snow, feeding currents, sinking aggregates, tracking microscopy

Authors for correspondence:

Deepak Krishnamurthy
e-mail: dkrishnamurthy@
schmidtsciencefelows.org
Rachel Pepper
e-mail: rpepper@pugetsound.edu

[†]These authors contributed equally to the study.

Electronic supplementary material is available online at https://doi.org/10.6084/m9.figshare. c.6384910.

THE ROYAL SOCIETY

Active sinking particles: sessile suspension feeders significantly alter the flow and transport to sinking aggregates

Deepak Krishnamurthy^{12,†}, Rachel Pepper^{3,†} and Manu Prakash²

¹Department of Bioengineering, University of California, Berkeley, USA ²Department of Bioengineering, Stanford University, Stanford, CA, USA ³Department of Physics, University of Puget Sound, Tacoma, WA, USA

(i) DK, 0000-0002-4504-1530; RP, 0000-0001-6804-8965; MP, 0000-0002-8046-8388

Sinking or sedimentation of biological aggregates plays a critical role in carbon sequestration in the ocean and in vertical material fluxes in wastewater treatment plants. In both these contexts, the sinking aggregates are 'active', since they are biological hot-spots and are densely colonized by microorganisms including bacteria and sessile protists, some of which generate feeding currents. However, the effect of these feeding currents on the sinking rates, trajectories and mass transfer to these 'active sinking particles' has not previously been studied. Here, we use a novel scale-free vertical tracking microscope (a.k.a. gravity machine; Krishnamurthy et al. 2020 Nat. Methods 17, 1040-1051 (doi:10.1038/s41592-020-0924-7)) to follow model sinking aggregates (agar spheres) with attached protists (Vorticella convallaria), sinking over long distances while simultaneously measuring local flows. We find that activity due to attached V. convallaria causes significant changes to the flow around aggregates in a dynamic manner and reshapes mass transport boundary layers. Further, we find that activity-mediated local flows along with sinking modify the encounter and plume cross-sections of the aggregate and induce sustained aggregate rotations. Overall, our work shows the important role of biological activity in shaping the near-field flows around aggregates with potentially important effects on aggregate fate and material fluxes.

1. Introduction

Suspended aggregates are key parts of natural and man-made aquatic ecosystems. In particular, macroaggregates (greater than 500 µm), known as marine snow, lake snow and river snow, can dominate nutrient, carbon and element cycling in aquatic environments [1-7]. In the ocean, marine snow aggregates are primarily responsible for vertical material fluxes from the surface mixed layer to the deep ocean, thus playing a critical role in marine carbon sequestration [1,5,6]. Similar aggregates are also a key part of activated sludge wastewater treatment facilities, where the sinking out of flocs is one of the main methods for removing organic debris and contaminants from the water [8]. Understanding aggregation rates, degradation rates, sinking speeds and composition of aggregates in aquatic environments is critical for understanding vertical fluxes of carbon and nutrients in these diverse ecosystems [1,7,9]. These rates can, in turn, depend on several biotic and abiotic factors. The local hydrodynamic environment of the sinking aggregate is one such factor: encounter rates, which determine particle size distributions and, thus, sinking rates, can depend sensitively on fluid flow near the aggregate, e.g. local shear, or the flow regime [9,10].

In marine, freshwater and waste-water contexts suspended aggregates are biological hot-spots: they are highly enriched in carbon and other nutrients, compared with the surrounding water, and are, therefore, an important micro-habitat for aquatic organisms [2,7,11–14] (figure 1a–c). Marine and freshwater aggregates are typically densely colonized by bacteria, flagellates and

Figure 1. 'Active sinking particles' in natural and man-made ecosystems. (a) A snapshot of a natural marine aggregate including a diatom chain (green arrow) colonized by suspension feeders (red arrows). (b) A freshwater aggregate colonized by various suspension feeders including Vorticella species, Stentor coeruleus and flagellates, such as Bodo species [15]. Image from Zimmerman-Timm et al. [15]. (c) An aggregate from the Tacoma Central Wastewater Treatment Plant showing dense colonization by suspension feeding microorganisms. (d) The examples in (a)–(c) constitute 'active sinking particles' wherein the aggregate's flow and mass transport characteristics have contributions both due to sinking as well as the active flows created by sessile microorganisms. The ratio of the effects of activity and sinking can be parametrized by the dimensionless ratio: A $\frac{1}{2}$ nF=DrVg, where n is the number of active entities (V. convallaria in our study), F is the force exerted on the fluid due to each active entity, $\Delta \rho$ is the density mismatch between the aggregate and fluid, V is the aggregate volume and g is the acceleration due to gravity.

ciliates, and are consumed by larger zooplankton [2,7,11,13,15]. Similarly, wastewater flocs are also densely colonized by bacteria and protists [16]. Sessile ciliates attached to flocs are especially important for effective wastewater treatment, and the particular species composition is used as an indicator of the stage and health of the effluent [16,17].

Downloaded from https://royalsocietypublishing.org/ on 08 February 2023

These attached organisms have been shown to affect aggregates by remineralizing carbon [2], but they may also affect aggregate properties by changing the local hydrodynamics around the aggregate. Many of the organisms found on aggregates, including protists and nanoflagellates, generate a feeding current to draw in food from the surrounding fluid [7,13,15,18]. These feeding currents can have velocities of the same order as near-field flows due to sinking (typical feeding current velocities 0.1-1 mm s⁻¹ [19,20] and sinking speeds of aggregates O(1 mm s⁻¹) [18]). We term these aggregates 'active sinking particles', with the local flow fields determined both by sinking and biologically generated flows. It is important to understand how this combination of sinking and biological activity affects mass transport, encounter rates with other aggregates, colonization of bacteria and other suspension feeders, as well as growth, degradation and sinking rates, yet these questions have not been systematically investigated so far. We have found only two studies that explore this potentially important

phenomenon. In the first study, the feeding currents of attached nanoflagellates were shown to dramatically increase aggregation rates for small (less than 20 µm) particles, but direct measurement of flows are needed to confirm the mechanism and to extend to both larger organisms and larger aggregates [18]. In another study, attached filter feeders were shown to increase mass transfer rates to stationary (not sinking) diatom cells at rates comparable to mass transfer rate increases due to sinking alone [21]. It has also been hypothesized that Vorticella that densely colonize buoyant cyanobacteria colonies may, similarly, improve the colonies' access to nutrients, though, as far as we are aware, this has not been further studied [22]. Despite their potential importance, the flows due to a combination of both sinking and biological activity have never been measured experimentally. This is a key missing piece, since this combination of sinking and biological flows probably has non-trivial effects due to the sensitive dependence of mass transport rates on streamline topology in the convection-dominated limit [23,24].

The sinking of and mass transport to 'active sinking particles' in their ecological context is a complex, multi-scaled process. For instance, millimetre scale marine snow particles sink at rates of the order of hundreds of metres a day while undergoing myriad transformations due to both physical and biological influences [5,25,26]. In situ measurements of such processes are naturally challenging, and earlier efforts

in the laboratory have used techniques including tethering aggregates and using a fixed background flow to simulate freely sinking conditions [6,27]. However, practical constraints posed by these experimental set-ups have made it challenging to bring modern microscopy techniques into the realm of this problem. Direct, real-time observations of near-field flows (single cell to aggregate scale), as well as dynamics of freely sinking aggregates, over both short and long time scales, are currently lacking.

In this work, we present a novel experimental system and measurements combining agar aggregates colonized by Vorticella convallaria (our model 'active sinking particles'), and scale-free vertical tracking microscopy (SVTM), a.k.a. gravity machine [28]. This recent advance in tracking microscopy allows freely sinking particles to be automatically tracked using a circular 'hydrodynamic treadmill'. Using this novel method we present the first detailed measurements and characterizations of near-field flows around 'active sinking particles' and find that they can be significantly modified by the presence of one or more V. convallaria cells. We also find that V. convallaria modify aggregate dynamics by causing sustained rotations, with implications for mass transport and aggregate transformations over long times. Finally, we show how the presence of one or more V. convallaria can affect aspects of mass transport to the aggregate including the encounter region and plume cross-sections, important parameters in estimating mass transport and aggregate growth and degradation rates. Overall, our work highlights the importance of biological activity in shaping the near-field flows and mass transport to sinking aggregates.

2. Material and methods

2.1. Experimental system

To study the multi-scale process of microscale near-field flows and macroscale sinking dynamics we leveraged SVTM [28] that uses controlled rotation of a circular 'hydrodynamic treadmill' to automatically keep small objects centred in the microscope field-of-view while allowing free movement with no bounds along the axis of gravity (figure 2a,b). SVTM allowed us to concurrently measure aggregate trajectories over metres (figure 2c), and capture images through video-microscopy at rates of 100 frames s¹ (figure 2d,e, electronic supplementary material, movie S1). The optical resolution of the imaging system was approximately 1 µm, thus enabling resolution of flows and dynamics at the scale of single cells colonizing the aggregate (figure 2e). We observed sinking spherical millimetre scale aggregates that were either bare or had one to several attached V. convallaria, a common species of sessile ciliates. Vorticella species are found abundantly on sinking aggregates in marine, freshwater and man-made ecosystems [15,16]. We then measured flow around active sinking particles using both particle image velocimetry (PIV) and particle path-line traces on short video segments.

2.2. Model sinking aggregates

We created simple model aggregates that share many of the properties of natural aggregates. In nature, macroaggregates are composed of aggregated biological and other debris and range in size from 0.5 mm to several centimetres [1,2,5]. Aggregates are typically smaller in estuaries and other areas of high shear (less than 2 mm) [2]. In all aquatic environments, aggregates are amorphous and fragile, have varied shapes and are typically highly porous [1,2,5,6]. Aggregate sinking rates range from less

than 1 m d⁻¹ to hundreds of m d⁻¹, with larger particles sinking faster [2,5].

We created approximately spherical particles from 0.3% agarose gel by dripping hot agar into a layer of oil as described in Cronenberg & Van den Heuvel [29]. We used vegetable oil rather than kerosene and also made particles of various sizes by directly touching drops to the oil surface while still attached to the syringe needle tip. This density of gel resulted in spheres that sank at velocities within the range observed for similarly sized marine snow [5]. We next incubated these gel particles overnight in cultures of V. convallaria, which were cultured as described in Vacchiano et al. [30]. We determined the number of V. convallaria cells per aggregate by counting them in the microscopy images obtained during SVTM.

2.3. Flow measurement

We measured flow around active sinking particles using PIV on short video segments. The water surrounding the spheres was seeded with 2 μm polystyrene spheres (Polysciences 19814). PIV analysis was performed using PIVlab [31]. The aggregates were masked manually; we then used a multi-pass PIV algorithm with decreasing size of the interrogation windows from 128 128 pixels to a final window size of 64 64 pixels with 50% overlap. Flow fields were then time-averaged over the length of the video (typically, between 1 and 2 s).

We selected a subset of our particles to analyse that were either bare of V. convallaria, or that had V. convallaria in focus and with feeding currents primarily directed in the focal plane. We also chose to analyse only video segments where the focal plane coincided with the centre of the aggregate in the depth dimension. These choices minimized out-of-plane flow, so that most of the flows of interest could be measured. As a result of these choices, we analysed flow fields for 12 video segments across seven different aggregates (details in electronic supplementary material, section S1.1). Aggregates ranged in diameter from 0.70 to 1.2 mm (mean of 0.97 mm), had sinking speeds of 0.2-5 mm s⁻¹ (mean of 3 mm s⁻¹), and Reynolds numbers of 0.2-0.5 (mean of 0.3). Details of each aggregate are in electronic supplementary material, section S1.1, and PIV results for all measured flow fields are available in a Dryad data repository [32], and the analysis code in a GitHub repository [33].

For obtaining particle path lines, the images were first registered using the Registration plugin in ImageJ [34] to stabilize small movements relative to the camera. The path lines were then obtained using the FlowTrace plugin for ImageJ [35] by taking the maximum intensity projection of images over a 1 s interval.

2.4. Widths of encounter region and plume

Using our measured flow fields, we estimated the width of the plume left behind by the aggregate as well as the width of the encounter region below the aggregate by following streamlines. The encounter region below a sinking aggregate is the volume of fluid where particles will, eventually, come into contact with the aggregate as it falls through the water column; the size and shape of this region is important for determining particle aggregation rates [10]. The plume is a volume of higher solute concentration left behind the aggregate as it sinks; bacteria and zooplankton may use the plume to find and colonize (or consume) sinking aggregates [6,7,36-38]. Following streamlines is a reasonable first approach, because the Péclet number (Pe) for these processes is much greater than one, indicating that flow dominates over diffusion in most situations. In the plume, concentrations of small molecules like oxygen and organic solutes, as well as of motile and non-motile bacteria can be increased or decreased by the presence of the aggregate. Diffusion con-stants for these can range from 10^{-9} (for oxygen and organic

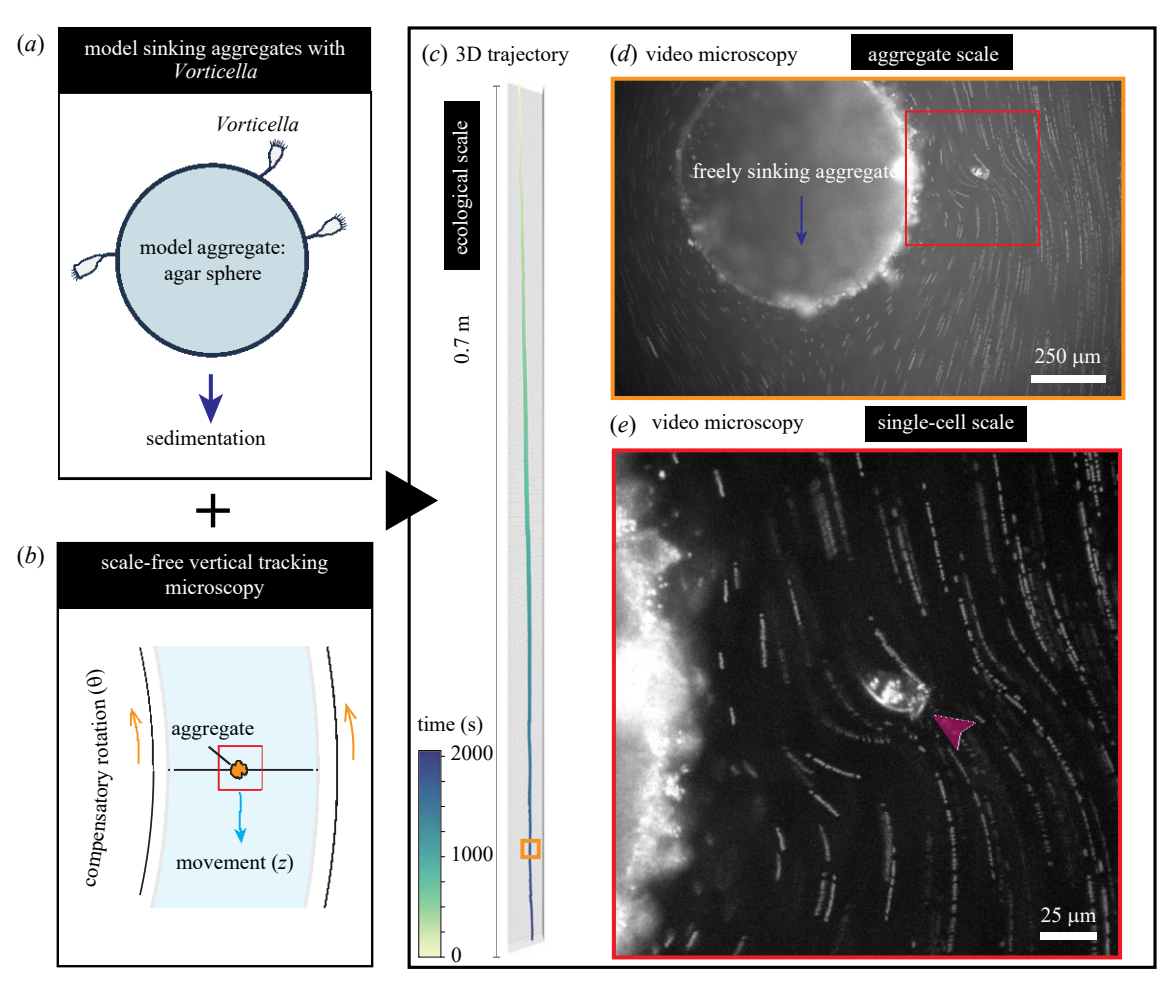


Figure 2. Scale-free vertical tracking microscopy of freely sinking model aggregates with attached Vorticella. (a) Model sinking aggregates comprising of agar spheres of radius approximately 0.5 mm and sedimentation speed of approximately 1 mm s⁻¹, colonized by V. convallaria. (b) Scale-free tracking microscopy using a 'hydrodynamic treadmill' allows multi-scale tracking of aggregates: observations are made at microscale resolution while concurrently allowing free sinking and tracking over macroscales (schematic, not to scale). (c) A typical three-dimensional trajectory of an aggregate showing sinking over 0.7 m in 33 min. In general, this multi-scale tracking method results in tracks where the spatio-temporal resolution is micrometres and milliseconds while the track extends over metres and hours. (d) Concurrent microscopy images of the aggregate captured in real time at a rate of 30 Hz, showing the aggregate and sessile suspension feeder. The photo corresponds to the orange box shown in (c). (e) Close-up view of the Vorticella cell demonstrating the fine optical resolution of the system. Arrow indicates the orientation of the cell and equivalently the direction in which stress is applied to the fluid.

solutes) to 10^{-14} m² s⁻¹ (for large non-motile bacteria), with motile bacteria falling in between [6,39,40]. Therefore, plume Péclet numbers for our aggregates are approximately $150-10^7$. The Sherwood number, defined as the ratio of total mass transport to mass transport from diffusion alone is also an important indicator of the relative importance of advection and diffusion around a sinking aggregate. For bare sinking spheres of similar Reynolds number to ours, the Sherwood number is 5 for Pe Oð 10^2 P and 10 for Pe Oð 10^4 P, again indicating that advection dominates over diffusion at this scale [6].

When considering the encounter region below the sphere, advection is even more dominant, and the Péclet number even higher. For instance, considering the encounter rate with a 100 μ m sphere, the Stokes–Einstein relation gives $D=2\times10^{-15}~\text{m}^2~\text{s}^{-1}$ with a resulting Péclet number of 10^8 [41].

When finding the plume width, we started streamlines in a ring around the aggregate at a distance of 140 μm from the aggregate surface and integrated forward in time in the measured flow field (figure 4). Streamlines that approached within 16 pixels (35 μm) of the aggregate surface were terminated, as the flow field measurement is noisy in this region. The width of the plume at each height above the aggregate is the distance between the outer-most streamlines (yellow line in figure 4). Here, choosing a distance of 140 μm from the aggregate surface can be considered choosing an approximate diffusion constant for the substance of interest: from a scaling perspective, the substance

will diffuse approximately 140 μm in the time it takes the aggregate to sink its own diameter. This yields D \square 10⁻⁹ m² s⁻¹, appropriate for oxygen or small organic solutes.

Similarly, we estimated the width of the encounter region below the aggregate, following the ideas in Humphries [10]. Particles within this region of fluid would come into contact with the aggregate as it falls through the water column. Similar to our plume calculation, we determined streamlines that began in a ring around the aggregate at a distance of 140 $\,\mu m$ from the aggregate surface. To find the encounter region, we then integrated backward in time in the measured flow field. The width of the encounter region is the distance between outer-most streamlines (equivalent to $2\times\lambda$ in Humphries [10], fig. 2). Choosing a beginning location of 140 $\,\mu m$ from the aggregate surface effectively gives the encounter region for particles in the water column that are 140 $\,\mu m$ or larger.

We compared our measured plume and encounter region widths with the known results for Stokes flow and Oseen's modification to Stokes flow ([42] eqns. (4.9.12) and (4.10.3)), where the Oseen flow was calculated for Reynolds numbers that matched parameters for each individual aggregate (see electronic supplementary material, table S1). Stokes flow is accurate for zero Reynolds number, while Oseen flow makes adjustments for Reynolds numbers close to one [42].

For more direct comparison with work such as Humphries and with theoretical coagulation kernels [9,10], we extended our experimentally measured streamlines beyond the field-of-

view of our experiments to a final vertical distance above and below the sphere of 20 times the particle radius (20a) using Oseen flow around a sinking sphere. We began the theoretical streamlines at the location of our experimentally measured streamlines when they were a vertical distance of 2a above or below the middle of the sphere (above for plume measurements and below for encounter region). The width of the plume at 20a was, then, the distance between the outer-most theoretical streamlines. These long-distance widths were only calculated for particles where the distance 2a was in the field-of-view (N = 9 for encounter volume and N = 10 for plume). Following Humphries [10], we also calculated long-distance widths of encounter regions and plumes using Oseen flow only (no input from experimental measurements) to compare experimental widths with theoretical widths for aggregates with the same size and sinking speed, but no attached V. convallaria.

Because of the low sample size, our flow field, and resulting plume and encounter region results, are a subset of what is possible with attached organisms, and probably do not show the full range of possible outcomes. Other results, such as the increased variation in encounter rate with increasing number of organisms and the rotation rate results, were found to be statistically significant, even with our low sample size, and can be considered representative results that would probably be reproducible in future experiments.

3. Results

3.1. Conceptual framework

Active sinking particles lie on the continuum spanned, on the one hand, by passive sinking particles that have no biological activity, and, on the other, by active swimmers under the influence of gravity (figure 1). This continuum can be parametrized by a non-dimensional ratio of forces due to activity and buoyancy. The active forces scale as nF where n is the number of active entities (Vorticella in our case) whose influence on the fluid is approximated as point forces (Stokeslets) of strength F [43]. The buoyant force due to gravity scales as $\Delta \rho Vg$ where $\Delta \rho$ is the density mismatch between the particle and ambient fluid, g is the acceleration due to gravity and V is the aggregate volume. The dimensionless ratio of active and buoyant forces is given by: A ¼ nF=DrVg. Using this parametrization, passive sinking particles have A ¼ 0, active swimmers are typically characterized by A * 1, while active sinking particles have 0, A & 1 (figure 1d). The value of A for some representative aggregates are shown in table 1.

3.2. Vorticella convallaria modify near-field flow and reshape boundary layers

We found that attached V. convallaria substantially changed the flows near sinking aggregates in ways that were variable and depended sensitively on the location and orientation of the attached organisms (representative examples in figure 3; all measured flow fields in electronic supplementary material, figure S1; N=12). A typical bare aggregate had relatively smooth flow (figure 3a,b) and both perpendicular and parallel flow near the particle that was similar to the predictions of flow at zero Reynolds number around a sphere of the same size (figure 3c, electronic supplementary material, movie S2). As expected, tangential flow was fastest at the equator, and radial flow was fastest at the poles (figure 3c).

On the other hand, figure 3 also shows two aggregates, each with three V. convallaria attached at random locations across the sphere, where the flow was modified by the V. convallaria. In figure 3d-f, the modifications to the flow were somewhat subtle: streamlines were pulled toward the V. convallaria, disrupting the background flow (figure 3d-f, supplementary material, movie S3). electronic V. convallaria in the bottom left, which was pulling fluid towards the particle, increased the radial flow and caused the tangential flow to be reduced on one side of the organism and enhanced on the other side (figure 3f). The cell near the north pole changed the local flow from primarily radial to primarily tangential (figure 3f). Since the V. convallaria altered the flow velocities and gradients near the sphere, they will cause the transport boundary layer to be thicker in some regions of the sphere (where velocities were reduced), and to be thinner in others (where velocities were increased). These changes were more substantial and widespread than smaller scale changes induced by irregularities on the surface of a bare aggregate (figure 3c). In figure 3g-i, the modifications to the flow by the V. convallaria were more dramatic: organisms on this aggregate caused largescale eddies, which changed the flow structure, completely altering tangential and radial flow velocities near the sphere (figure 3g-i, electronic supplementary material, movie S3). In some regions, the flow direction was even reversed from what it would have been for a bare sinking aggregate (figure 3i). Again, the boundary layer near this sphere was substantially reshaped in ways that would change both total mass transport to the sphere and which regions of the sphere have the highest rates of mass transfer. These effects on the flow field were even more dramatic for larger numbers of V. convallaria (greater than three) (electronic supplementary material, movie S4), though we had fewer examples of such aggregates in our experiments. Such diversity of flow structures caused by V. convallaria feeding flow is similar to that observed and predicted previously for Vorticella, and similar organisms, attached to surfaces and in ambient flow [20,39,43,48]. In still water next to a wall, the Vorticella feeding current consists of a toroidal eddy when the cell body is perpendicular to the surface, but flow that does not recirculate at other orientations [39,48]. In flowing water, there is recircula-

Other experimentally measured flow fields are shown in electronic supplementary material, figure S1, and original PIV flow field data for all included flow fields are available in a Dryad data repository [32].

tion when the organism pushes against the ambient flow [43].

To understand the relative effects of activity and sinking on mass transport from the aggregates, we can compare their relative contributions with the velocity within the mass transport boundary-layer. Advective effects of the flow dominate diffusive effects for the range of aggregate sizes, sinking speeds and even for transport of small molecules such as oxygen from the aggregate (Material and methods). This implies that the non-dimensional Péclet number (Pe=Ua/D), which quantifies the relative importance of these effects, is much greater than 1 (Material and methods). Here, U is velocity scale of the flow, a is the aggregate radius and D is the diffusivity of the molecule of interest. At such high Péclet number, the mass transport boundary layer is a thin region near the aggregate whose thickness is approximately aPe-1/3 [49]. The hydrodynamic effect of V. convallaria on the fluid can be modelled as a point-force

Table 1. Sample estimates of activity versus sinking effects for natural and man-made active sinking particles showing type of organisms found colonizing and typical numbers. These parameters are used for calculating A ¼ nF=DrVg. The calculation is done considering only a single species and is hence a conservative minimum estimate. The density mismatch between aggregate and the surrounding fluid is calculated using scaling laws from Alldredge & Gotschalk [44] if not reported in the original reference. The point forces due to organisms used were approximately 2 pN for choanoflagelates [45], approximately 10 pN for nanoflagelates [46] and approximately 200 pN for V. convallaria [43] and Vorticella sp. [22].

type of aggregate	size (mm)	colonizing organism	number (n)	А	reference
marine	10	choanoflagellates	10 ⁵	0.86	[47]
freshwater	1	nanoflagellates	25	0.027	[15]
freshwater	0.2	Vorticella sp.	20	4.5	[22]
wastewater	1	V. convallaria	10	0.12	this work

of magnitude F at a height h above the boundary [43]. The velocity scale due to Vorticella within this boundary layer is then F/ μ h. On the other hand, the velocity scale within the boundary layer due to sinking is OđUPe¹⁻³p. Comparing these two scales in the vicinity of a Vorticella cell we obtain a critical sinking speed that separates the 'activity-controlled' and 'sinking-controlled' mass transport regimes,

For sinking speeds above this scale, sinking is expected to dominate mass transport. Note that this picture is local, and the overall effect of the mass transport will depend on the number of Vorticella, as well as their orientation relative to the sinking direction of the aggregate. For instance, when Vorticella are oriented parallel to the local flow they can cause local flow reversals that completely disrupt the boundary layer structure and cause it to lift off the aggregate surface (see, for instance, figure 3g,h). Based on the measured parameters for V. convallaria (F ¼ 200 pN, h 2 100 μm; [39]), aggregate size a = 0.5 mm, and considering the transport of biologically relevant small molecules like oxygen $(D = 10^{-9} \text{ m}^2 \text{ s}^{-1})$, we obtain $U_{\text{critical}} = 63 \text{ mm s}^{-1}$. This number is much higher than the sinking speeds in our experiments (which, in turn, are representative of sinking speeds of real aggregates), indicating that activity probably dominates mass transport locally (see table 2).

3.3. Vorticella modify encounter region and plume width

We find that attached V. convallaria significantly modify both the region of encounter below sinking aggregates and the shape of the plume left behind (figure 4). Our aggregates show that bare spheres have encounter regions and plumes fairly close to those predicted by Stokes and Oseen flow (figure 4a), while those with V. convallaria have plumes and encounter regions with significant asymmetry and that can be both narrower and wider than those of bare spheres (figure 4b-e). Changes are particularly dramatic when the Vorticella cause recirculation in the flow (figure 4c-e). When extrapolated to distances far from the sphere (more details in Material and methods), we find that the width of the region encountered by the sphere and the width of the plume left behind are significantly changed by attached organisms, and that these changes lead to both thicker and thinner plumes and wider and narrower encounter regions (figure 4f,g). Each

of our measurements are at a single time point and measure a two-dimensional cross-section of a three-dimensional flow. It is, therefore, possible, for instance, that in some cases attached V. convallaria cause the plume to be thinner in one dimension while thicker in another. Also, these changes are likely to be dynamic in time, leading to e.g. a sometimes wider encounter region and sometimes narrower as time passes and V. convallaria orientations and positions on the aggregate change.

We also used our long-distance encounter-width measurements (figure 4g) to predict how attached organisms change particle coagulation kernels. Particle encounter dynamics are included in aggregation models through the coagulation kernel that expresses encounter rate (in volume/time) [9]. The two most commonly used kernels are the rectilinear kernel,

$$b_{rec}$$
 ¼ p δr_i b r_i P 2 j u_i u_i j, $\delta 3:2$ P

and the curvilinear kernel.

where r_i is the radius of the larger particle (here the sinking agar sphere), r_j is the radius of the smaller particle (here assumed to be 140 μ m for simplicity—see Material and methods for further details), and u_i and u_j are the sinking speeds of the two particles [9]. The rectilinear kernel does not include any distortion of the flow due to the presence of particles, the curvilinear kernel is more accurate and is based on the assumptions of Stokes flow [9]. If we assume our long-distance encounter widths (figure 4f) are axisymmetric, our experimental kernels would have the form,

$$b_{exp} \ ^{1/2} j u_i \ u_j j,$$
 $\delta 3:4$

where λ is half of the encounter width shown in figure 4f [10]. Using this formulation, we find that attached organisms lead to encounter kernels that are always smaller than the rectilinear kernels, and approximately $2\times$ to $10\times$ the curvilinear kernels (figure 4h).

It has previously been shown that including the finite size and sinking speed of particles (as opposed to assuming Stokes flow and zero Reynolds number) has a similar effect of increasing the size of encounter kernels [10]. We, therefore, also compared our experimental encounter kernels with those calculated theoretically from Oseen flow, by following the Oseen encounter regions (e.g. dashed orange lines in figure 4a–c), to long distances. Then,

$$b_{Oseen} \% pl_O^2 ju_i u_j j,$$
 $\delta 3:5P$

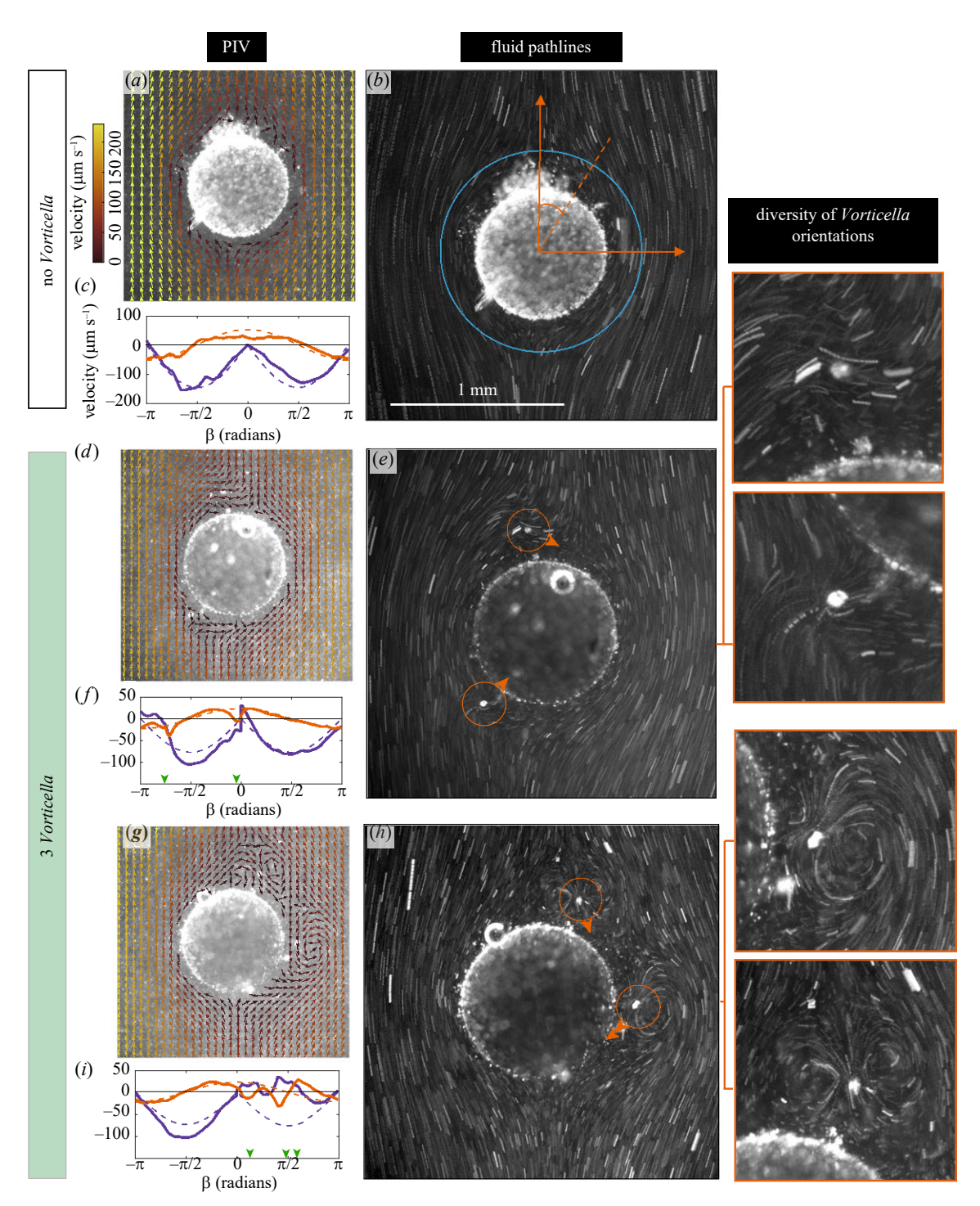


Figure 3. Flow around active sinking aggregates. Each row has measurements for a different sinking aggregate. (a,d,g) Measured flow velocities. Arrows indicate flow direction and colour indicates speed. (b,e,h) Path lines formed from tracer particles over approximately 1 s. Circles indicate location of Vorticella and arrows indicated the direction of Vorticella forcing. (c,f,i) Measured velocities (solid lines) along a circle 200 μ m from the sphere surface (e.g. blue line in (b)). β is the polar angle indicated in (b), and is positive to the right of the sphere and negative to the left. Perpendicular (red curves) and parallel (blue curves) components of the velocity are relative to the sphere surface. Dashed lines are calculated velocities for Stokes flow (zero Reynolds number) around a sphere of the same size. Green arrows show location of V. convallaria. Aggregate 1; top row; (a)—(c): no attached Vorticella; Aggregate 2; middle row; (d)—(f): three attached Vorticella (one out of view); Aggregate 3; bottom row; (g)—(i): three attached Vorticella. Aggregate parameters are shown in table 2.

Table 2. Parameters for aggregates in figure 3.

aggregate number	figure 3 panel	a (μm)	U (μm s ⁻¹)	Re
1	(a)–(c)	380	340	0.3
2	(d)–(f)	490	200	0.2
3	(g)–(i)	490	210	0.2

where $\lambda_{\rm O}$ is half of this theoretical long-distance encounter width [10].

We found that aggregates with attached V. convallaria had larger encounter kernels, compared with the Oseen kernel, than those without (figure 4i), and that this was more pronounced for aggregates with a larger number of attached V. convallaria, though this trend was not significant with our small sample size (linear regression model: $R^2 = 0.42$; p = 0.057), and with a larger sample size, we predict we

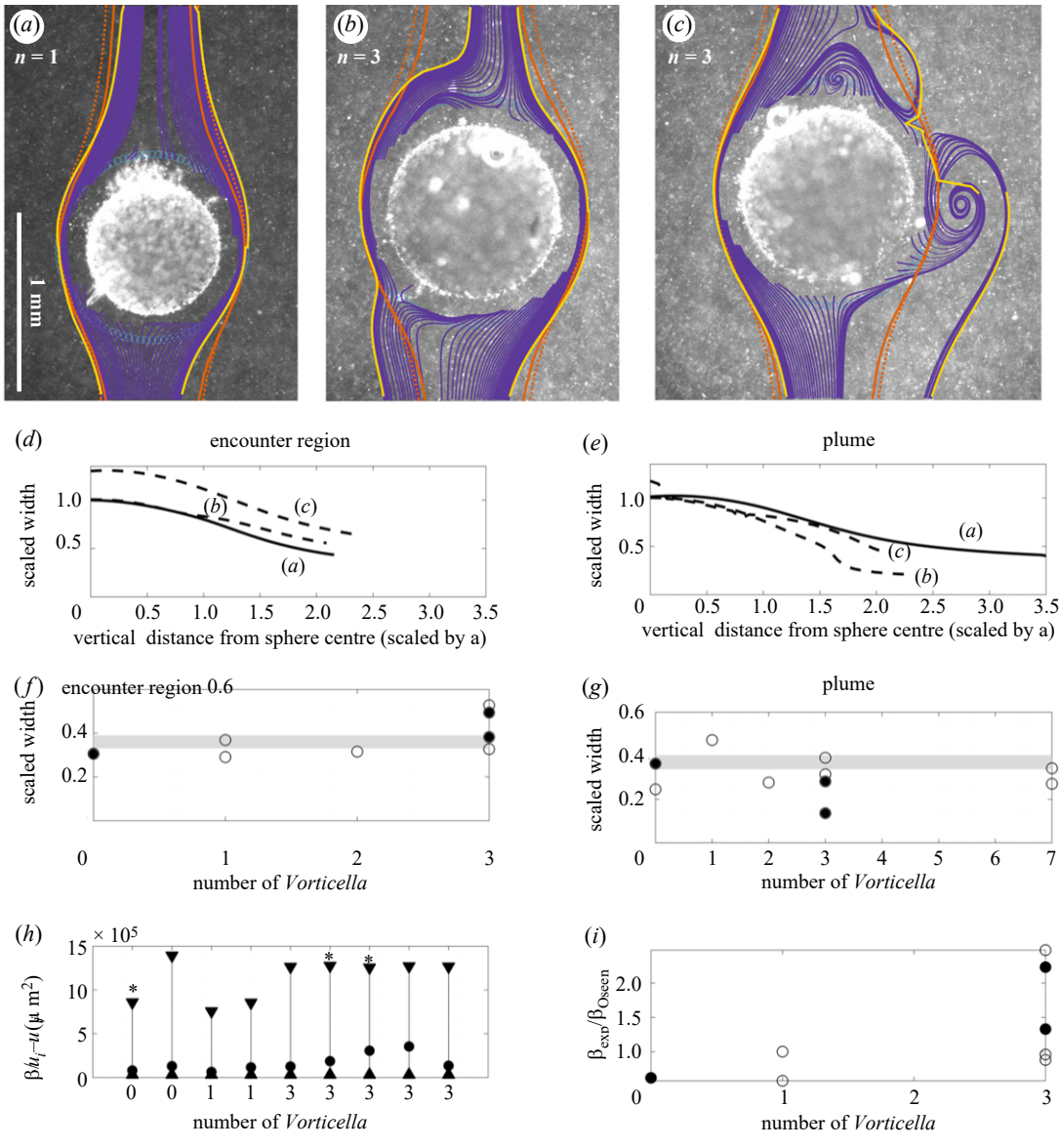


Figure 4. Encounter region and plume of sinking aggregates. (a—c) Streamlines around sinking aggregates (purple) calculated using experimentally measured flow fields. Streamlines begin in a ring around the aggregate (blue circles). Yellow lines indicates outer limits of these streamlines (e.g. the width of the plume and encounter region). Orange lines indicate theoretically calculated plume and encounter region widths. The solid lines indicate Stokes flow and dashed lines indicate Oseen flow. (d,e) Width of the intersection cross-section and plume for the aggregates in (a)—(c). Letters indicate which panel matches which line and the solid line indicates that no Vorticella are attached. Widths are scaled by initial width at the equator of the sphere. (f,g) Long-distance encounter cross-section and plume width (N = 9 for encounter region; N = 10 for plume). Solid circles indicate aggregates shown in (a)—(c) and shaded region indicates the range predicted by Oseen flow. (h,i) Particle coagulation kernels scaled by encounter velocity (N = 9). (h) The rectangular (upper triangles), experimental (circles) and curvilinear (lower triangles) kernels are compared for the parameters of each experimental aggregate. Stars indicate aggregates shown in (a)—(c). (i) The experimental coagulation kernel, β_{exp} , divided by the kernel for Oseen flow around a sphere of the same size and sinking speed, β_{Oseen} (N = 9). This indicates by how much encounter rates would be changed in our measured flow versus ideal bare spheres. Solid circles indicate aggregates shown in (a)—(c).

might also observe encounter kernels smaller than bare spheres. Perhaps more important, the variation in encounter kernel size compared with theoretical bare spheres increased with increasing number of attached organisms (figure 4i; Levene's test indicated unequal variances; F = 8.5, p = 0.018).

Downloaded from https://royalsocietypublishing.org/ on 08 February 2023

3.4. Vorticella convallaria cause sustained rotation of aggregates

Our novel experimental system enabled us to observe aggregates as they sank freely in the ambient fluid without the constraining influence of tethers or other attachments, required in earlier experimental systems [27]. We observed that freely sinking aggregates displayed sustained rotational motion correlated to the presence of V. convallaria (figure 5a,

electronic supplementary material, movie S5). To explore this quantitatively, we developed a custom image-processing pipeline (electronic supplementary material, section S1.2), and used tracked surface fiduciary markers naturally occurring on the aggregates to estimate rotation rates and three-dimensional rotation axes from the two-dimensional images generated by SVTM. We find that aggregates without V. convallaria show little to no rotation (figure 5a). On the other hand, aggregates colonized by one or more V. convallaria show sustained rotations that are visible by eye even over a 30 s interval (figure 5b). To explore if the number of organisms was the main driver of this rotation, we isolated the effects of aggregate size on the observed rotation rates by rescaling the rotation rate by the scaling factor $\[\] V$ $\[V_{\text{vorticella}} = 8 \] Pma^2$, where $\[V_{\text{vorticella}} = 8 \]$ is the force-scale exerted on the fluid by a single

royalsocietypublishing.org/journal/rsif

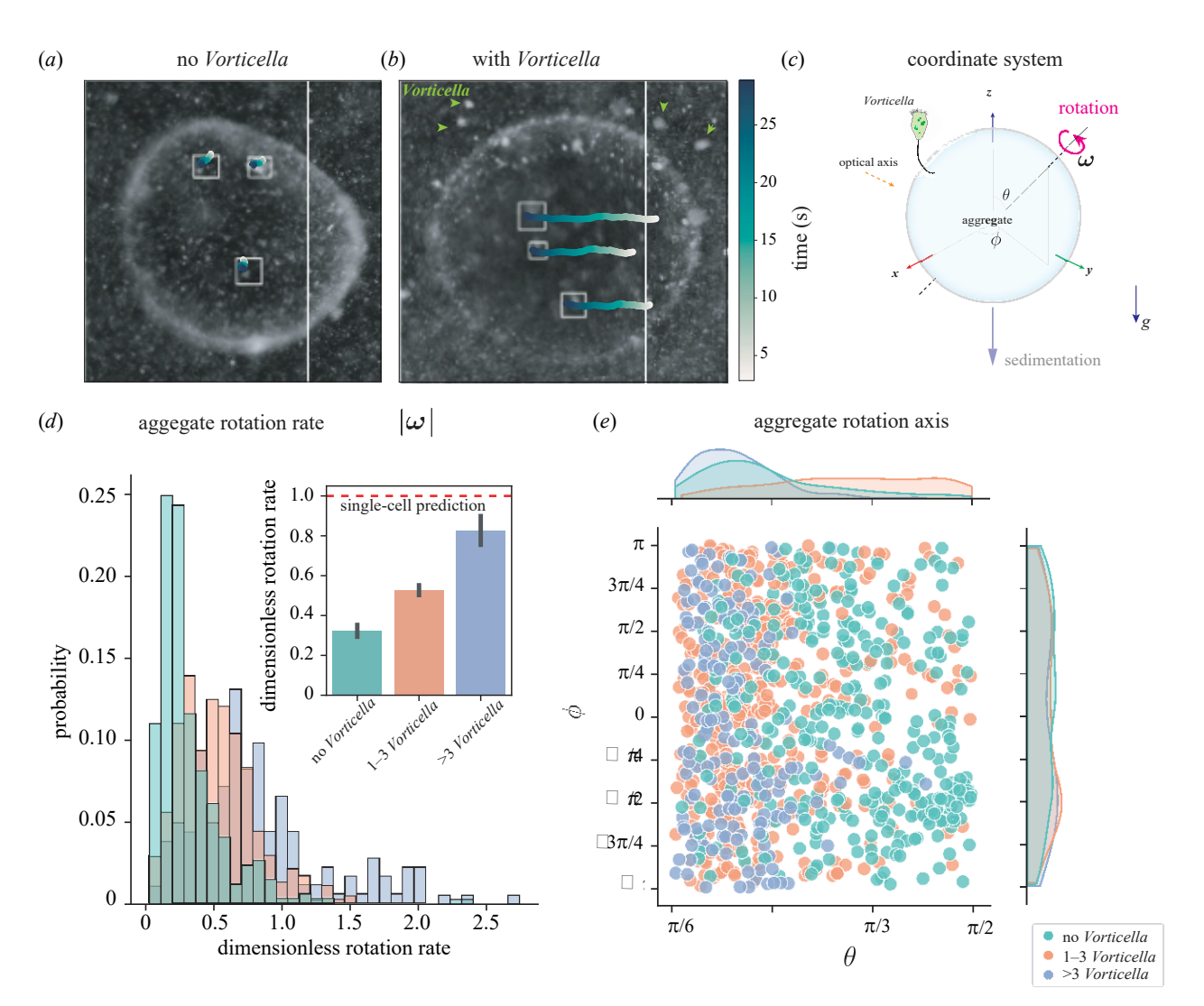


Figure 5. Effect of Vorticella on rotational dynamics of sinking aggregates. (a) and (b) Microscopy snapshots of aggregates without Vorticella and with n > 7 Vorticella, respectively, with tracks of surface features overlaid. Green arrows indicate Vorticella locations in (b). Tracked surface features show significant excursion in (b) due to the rotation of the aggregate. (c) Coordinate system for quantifying the rotational dynamics of aggregates. Aggregate rotation rate is defined by ω and the rotation axis by the polar and azimuthal angle pairs (θ, ϕ) , respectively. (d) Comparison of mean rotation rates of aggregates without and with Vorticella. Results are presented over N = 7 distinct aggregates for the 'no Vorticella' condition and over N = 6 aggregates for the 'with Vorticella' conditions. Aggregates with Vorticella show significantly larger rotation rates compared with those without Vorticella (Kruskal–Wallis test comparing the three conditions $\chi^2(3) = 257$, $p < 10^{-6}$). The red-dashed line shows the theoretical rotation rate for an aggregate based on a single Vorticella. (e) Joint distribution of the angles that define the axis of rotation. Aggregates with Vorticella tend to rotate about axes that are parallel to the axis of gravity.

V. convallaria cell (approx. 200 pN [43]), μ is the ambient fluid viscosity and a is the aggregate radius. This scaling factor corresponds to the theoretical rotation rate for a spherical aggregate with a single V. convallaria oriented tangential to the aggregate surface. Upon rescaling, we find that the mean dimensionless rotation rates are higher for aggregates with V. convallaria than for aggregates without (figure 5d; mean dimensionless rotation rate with no Vorticella: 0.32 ± 0.27 , 1–3 Vorticella: 0.53 ± 0.27 , and greater than 3 Vorticella: $0.82 \pm$ 0.50, the differences in mean rotation rates were found to be statistically significant based on the Kruskal-Wallis test $\chi^2(3) = 257$, $p < 10^{-6}$, N = 13 distinct aggregates). That the dimensionless rotation rate is Oolp further indicates that V. convallaria are indeed the driving factors behind the rotation (figure 5d, inset). We further confirmed that measured changes in rotation rates were best explained by V. convallaria numbers and not due to other experimental conditions (electronic supplementary material, figure S2). Interestingly, we found that not only does the mean rotation rate rise with V. convallaria number, but the fluctuations about the mean do as well,

with the distribution of higher V. convallaria numbers becoming heavy-tailed (figure 5d and inset). These results can be explained by the previously observed stochastic reorientation of V. convallaria body angle relative to the surface of attachment: V. convallaria reorient with a period of minutes, which could lead to a time-varying torque from each organism [43]. If these motions are uncoordinated among the various attached individuals, both the mean rates of rotation and largest rates of rotation increase with Vorticella number for small numbers of Vorticella, as we observe. Models, experiments with much larger numbers of Vorticella, or experiments in which Vorticella body angle was explicitly tracked, could reveal if there is any coordination among the organism (either actively, or passively through coupled flows).

We also find that V. convallaria induce rotations about specific axes that lie close to the axis of gravity, as evident in the distribution of the rotation axis over a unit sphere (figure 5c). The distribution is relatively uniform for the no Vorticella case, but with increased number of V. convallaria, the distribution peaks along the axis of gravity $(\theta = 0)$. We interpret this result as

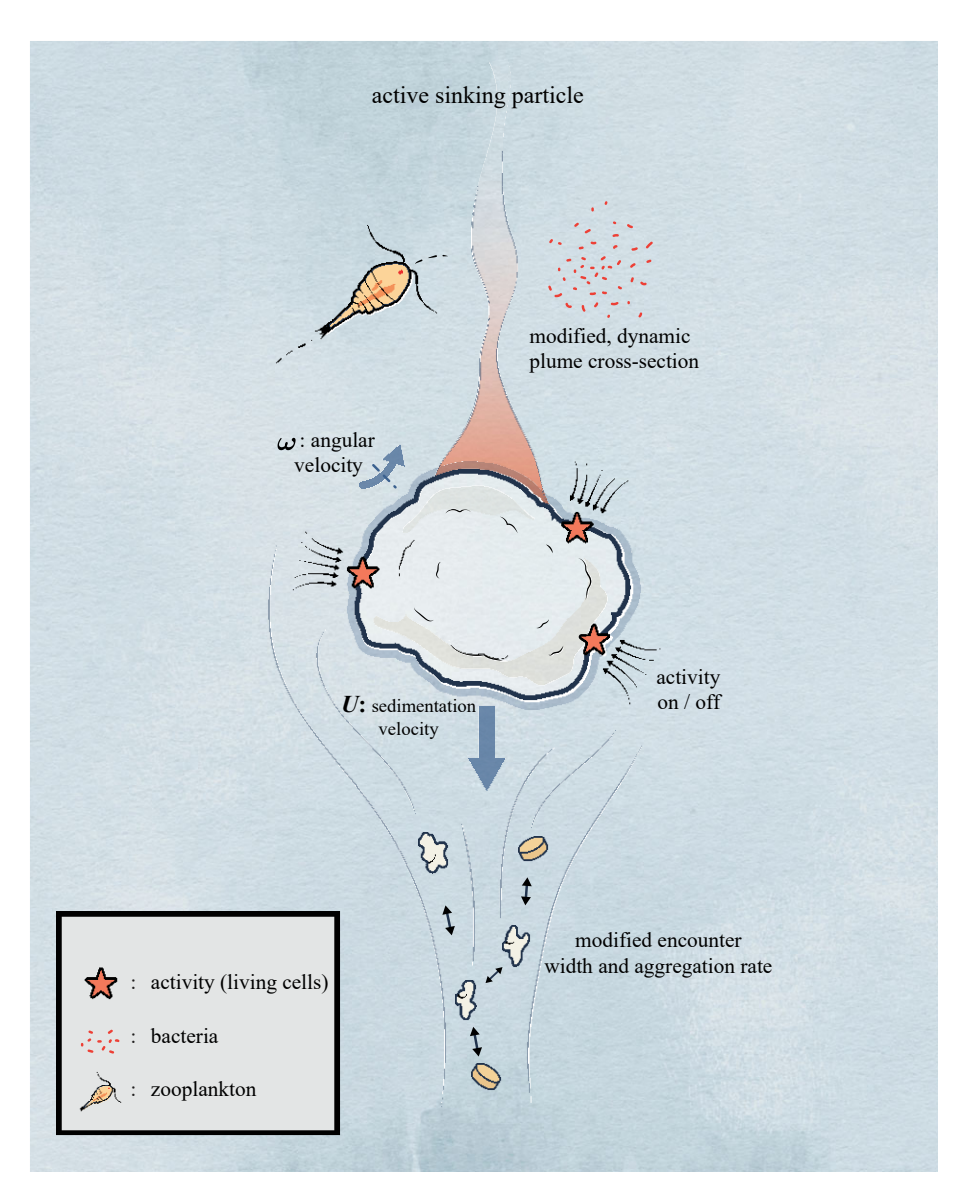


Figure 6. Our results support a new paradigm for 'active sinking particles', compared with the previous view of particles that passively sink with no active hydrodynamic interactions.

occurring due to gravity breaking symmetry in orientation space, wherein aggregates have a stable sedimentation orientation along the polar axis (θ) due to possible density distribution or shape effects, including the drag due to Vorticella, providing a stabilizing torque. Thus, the stochastic active torques due to V. convallaria cause the aggregate to sample orientation space along the azimuthal direction (ϕ) , as evidenced in our measurements.

4. Discussion and condusion

Our results suggest a new paradigm for how aquatic sinking aggregates interact hydrodynamically with their surroundings (figure 6). In the past, they have been viewed as passive particles, subject to the flow around them, whereas our results show that the flows generated by attached organisms change both aggregate local flow and sinking dynamics. Our results are a first step towards understanding the impact of this new paradigm, as the change we measure is likely to affect every aspect of these particles, including mass transport, the chemical signature they leave in their wake, and the aggregation, dissolution and settlement rates. Our work sets the stage for further detailed investigations of all these effects.

Previously, mass transport from small particles or aggregates has been studied in a wide range of flow conditions including uniform flow, shearing flows of different types and, finally, turbulent flow [49-53]. These works point to the crucial importance of near-field streamline topology in determining mass transfer (or heat transfer) rates at high Péclet numbers. As shown in this work by direct observation, organisms can change the near-field flow structures significantly, with the flow topology being dependent on the orientation of the activity. This probably leads to a different mass transfer rate scaling than both passive sinking and active swimming particles which scale as Pe^{1/3} and Pe^{1/2}, respectively [49,53]. This mass transport rate is also probably time-varying due to activity-induced rotation and will depend in a non-trivial way on the number and distribution of suspension feeders on the aggregate, making its estimation an interesting problem. While beyond the scope of this work, a general parametric model for active sinking particles which estimates this time-averaged mass transport rate as a function of aggregate parameters and suspension feeder density using theory-experiment dialogue would be an interesting future direction, and would directly inform ecosystem-scale models.

The importance of attached organisms' flow fields on mass transport was also recently studied in the case of organisms attached to stationary diatoms, wherein the activity induced flows significantly enhanced nutrient fluxes to a simulated stationary (not sinking) diatom cell [54]. Further, this enhancement was of a similar scale to that for sinking, assuming a similar density differential to our particles. These new results, thus, support our finding that even a few attached organisms can change the mass transport characteristics of sinking aggregates. We, therefore, anticipate that future investigations of the details of combined advection and diffusion to active sinking particles, and the resulting mass transport rate scaling, may reveal a complex interplay between passive sinking and active organism flows.

The above changes to mass transport rates would affect how active sinking particles interact with the water column at larger scales. One example of this would be through the plume left behind the particle. Such plumes are an important source of nutrients for microbial life in the water column and may attract both bacteria [36] and larger organisms like copepods to sinking particles [7,37,38]. As shown here, activity significantly modifies the plume cross-section, thus impacting the chances of encounter by bacteria and copepods. In the future, direct visualization of the plume using fluorescent dyes and SVTM in both model and natural aggregates would be an interesting study.

Another example of changes to particles' interaction with the water column at larger scales is mediated by changes to encounter rates. Studies have shown that changes in nearfield flows can substantially change encounter rates of sinking aggregates with each other [9,10]. When combined with coagulation models, moderate changes in encounter dynamics can have large-scale changes on the size spectrum of sinking aggregates as a function of depth [55,56]. Changes in this size spectrum further significantly change model predictions of carbon sequestration and export to the deep ocean, as well as biogeochemical and trace element distributions in aquatic ecosystems [9,55,56]. We find that attached organisms lead to encounter kernels that are always smaller than the rectilinear kernel, approximately $2 \times$ to $10 \times$ the curvilinear kernel, and are more variable than those for bare spheres without attached organism. Experimental measurements of particle encounter rates indicate that true coagulation kernels are, indeed, between the rectilinear and curvilinear kernels [9,57,58]. This discrepancy has been attributed to porosity, fractal geometry and intermediate Reynolds number flow [10,57,58]. However, our results show that flow from attached organisms could also be a key explanatory factor for this discrepancy. Thus, fully accounting for organism-generated flows may be important for creating accurate models of particle encounters and size spectra in aquatic ecosystems.

Attachment to sinking aggregates also probably affects the feeding rates of the attached organisms. Attaching to a sinking aggregate provides organisms with an environment enhanced in food [2,7,12–14] and also changes the hydrodynamics of feeding and organism clearance rates [59,60]. Changes in aggregate sinking and rotation rates due to the feeding currents of attached organisms, such as V. convallaria, could, in turn, have a further knock-on effect on the feeding rates of these organisms. For instance, a larger encounter cross-section due to the feeding currents of attached organisms could lead to enhanced aggregation and faster sinking rates. If organisms were able to orient downwards pointing into the flow, faster sinking

would lead to enhanced feeding [43]. However, if organisms were forced into unfavourable orientations, as suggested by Pepper et al., then faster sinking might reduce feeding rates [43]. Similarly, a reduced encounter cross-section, which we also find to be a potential consequence of feeding currents of attached Vorticella, would have the opposite effect. This means that the feeding rates of attached organisms may be more dynamic and variable than we would expect if we do not take these active effects into account. Similarly, the organism-induced rotation has been predicted to decrease mass transfer to sinking spheres due to curving or recirculating streamlines that cause water to spend more time in the vicinity of spheres [50,52]. This could lead to reduced feeding rates for attached organisms, but it is also possible that the interaction of the feeding currents with the rotation-induced flow could lead to increased feeding rates and mass transfer at some organism orientations or when the axis of rotation and rotation rate are dynamic in time. It would be fruitful to investigate these effects further using simulations and experiments to track feeding over time (e.g. [43,54]).

While our results clearly show that attached organisms fundamentally change how sinking aggregates interact hydrodynamically with their environment, our work is just the beginning in understanding both the details of this change and its full implications. Our results are two-dimensional cross-sections of complex three-dimensional flows; understanding the full three-dimensional flow either through experiment or theory/simulations is an important next step. Indeed, this is possible within the framework of SVTM by leveraging volumetric imaging techniques. Further, we study one size class of sinking aggregate with attached V. convallaria. Both larger and smaller aggregates are plentiful and important in aquatic ecosystem; similarly, smaller nanoflagellates are abundant on sinking aggregates and generate feeding flows on a smaller scale. Exploring these effects of size scaling of the organisms as well as aggregates is another important area for future investigation. For instance, while feeding flow was the dominant effect of Vorticella on the near-field flow of our aggregates, for smaller aggregates, numerous attached organisms could change the shape, size and density of the aggregate in ways that could also substantially change near-field flows and mass transport [22]. Further, our aggregates, while ideal for a first examination, may be different from real aggregates in several ways. It would be interesting and relevant to investigate how feeding currents of attached organisms interact differently with fractal and irregular aggregates as well as porous aggregates. Our experimental measurements can also serve to validate future flow simulations which can then be used in advection-diffusion models to more fully explore the effects of attached organisms on mass transport to sinking aggregates.

It has recently become increasingly clear that understanding microscale processes in aquatic systems is critical for accurately understanding ecosystem level processes [7,61–64]. Our results show that it is critical to understand the near-field flow contributions of attached organisms in order to accurately predict the role of sinking aggregates in aquatic ecosystems. By modifying encounter rates, attached organisms may help determine the particle size spectrum of sinking aggregates, and, thus, the many ecosystem processes mediated by aggregates. Similarly, by changing mass transport rates and plume characteristics, attached organisms may modify the composition of bacterial, nanoflagellate and protist

communities living on these aggregates, with follow-on effects on the balance of remineralization and sinking, and, therefore, the export rates of carbon and other nutrients to the deep ocean.

Data accessibility. Original PIV flow field data for all included flow fields are available from the Dryad data repository: https://doi.org/10. 5061/dryad.j6q573nf8 [32]. All the code used for data analysis and figure generation are shared on GitHub [33].

Supplementary material is available online [65].

Authors' contributions. D.K.: conceptualization, data curation, formal analysis, investigation, methodology, resources, software, validation, visualization, writing-original draft, writing-review and editing; R.P.: conceptualization, data curation, formal analysis, funding acquisition, investigation, methodology, resources, visualization, writingoriginal draft, writing-review and editing; M.P.: conceptualization, funding acquisition, methodology, resources, supervision, writingreview and editing.

All authors gave final approval for publication and agreed to be held accountable for the work performed therein.

Conflict of interest dedaration. We declare we have no competing interests. Funding D.K. acknowledges support from Bio-X Fellowship and Schmidt Science Fellowship. We thank Hopkins Marine Station for lab-space for experiments. We are also grateful for support from NSF grant no. IOS-1755326 to R.P. M.P. acknowledges financial support from NSF Career Award, Moore Foundation, HHMI Faculty Fellows Program, NSF CCC (DBI-1548297) Program, NSF Convergence Award (OCE-2049386), Schmidt Foundation and CZ BioHub Investigators Program.

Advowledgements. We thank Rebecca Konte for graphics and artwork in figures 1 and 6. We are grateful to A. Andersen, E. Riley and T. Kiørboe for helpful discussion. We also thank Rahul Chajwa, Hongquan Li and Prakash Lab members for valuable discussions. Thank you, also, to the Tacoma Central Wastewater Treatment Plant for help with wastewater samples, particularly K. Callier, M. Hoover, and F. Solorio.

References

- Alldredge AL, Silver MW. 1988 Characteristics, dynamics and significance of marine snow. Prog. Oceanogr. 20, 41-82. (doi:10.1016/0079-6611(88)90053-5)
- Simon M, Grossart HP, Schweitzer B, Ploug H. 2002 Microbial ecology of organic aggregates in aquatic ecosystems. Aquat. Microb. Ecol. 28, 175-211. (doi:10.3354/ame028175)
- Droppo IG, Ongley ED. 1994 Flocculation of suspended sediment in rivers of southeastern Canada. Water Res. 28, 1799-1809. (doi:10.1016/ 0043-1354(94)90253-4)
- Grossart HP, Simon M. 1993 Limnetic macroscopic organic aggregates (lake snow): occurrence, characteristics, and microbial dynamics in Lake Constance. Limnol. Oceanogr. 38, 532-546. (doi:10. 4319/lo.1993.38.3.0532)
- Alldredge AL, Gotschalk C. 1988 In situ settling behavior of marine snow. Limnol. Oceanogr. 33, 339-351. (doi:10.4319/lo.1988.33.3.0339)
- Kiørboe T, Ploug H, Thygesen UH. 2001 Fluid motion and solute distribution around sinking aggregates. I. Small-scale fluxes and heterogeneity of nutrients in the pelagic environment. Mar. Ecol. Prog. Ser. 211. 1-13.
- Kiørboe T. 2001 Formation and fate of marine snow. small-scale processes with large-scale implications. Sci. Mar. 65(Supp. 2), 57-71.
- 8. Srivastava A, Seo SH, Ko SR, Ahn CY, Ch HM. 2018 Bioflocculation in natural and engineered systems: current perspectives. Crit. Rev. Biotechnol. 38, 1176-1194. (doi:10.1080/07388551.2018.1451984)
- Burd AB, Jackson GA 2009 Particle aggregation. Annu. Rev. Mar. Sci. 1, 65-90. (doi:10.1146/ annurev.marine.010908.163904)
- 10. Humphries S. 2009 Filter feeders and plankton increase particle encounter rates through flow regime control. Proc. Natl Acad. Sci. USA 106, 7882-7887. (doi:10.1073/pnas. 0809063106)
- 11. Silver MW, Gowing MM, Brownlee DC, Corliss JO. 1984 Ciliated protozoa associated with oceanic

- sinking detritus. Nature 309, 246-248. (doi:10. 1038/309246a0)
- 12. Kiørboe T. 2000 Colonization of marine snow aggregates by invertebrate zooplankton: abundance, scaling, and possible role. Limnol. Oceanogr. 45, 479-484
- 13. Artolozaga I, Ayo B, Latatu A, Azúa I, Unanue M, Iriberri J. 2000 Spatial distribution of protists in the presence of macroaggregates in a marine system. FEIVS Microbiol. Ecol. 33, 191-196. (doi:10.1111/j. 1574-6941.2000.tb00741.x\
- 14. Stocker R. 2012 Marine microbes see a sea of gradients. Science 338, 628-633. (doi:10.1126/ science.1208929)
- 15. Zimmermann-Timm H, Holst H, Müller S, Muller S. 1998 Seasonal dynamics of aggregates and their typical biocoenosis in the Elbe estuary. Estuaries 21. 613. (doi:10.2307/1353299)
- 16. Water Environment Federation. 2017 Wastewater biology: the microlife, 3rd edn. Alexandria, VA: Water Environment Federation.
- 17. Foissner W. 2016 Protists as bioindicators in activated sludge: identification, ecology and future needs. Eur. J. Protistol. 55(Pt A), 75-94. (doi:10. 1016/j.ejop.2016.02.004)
- 18. Fukuda H, Koike I. 2000 Feeding currents of partide-attached nanoflagellates a novel mechanism for aggregation of submicron particles. Mar. Ecol. Prog. Ser. 202, 101-112. (doi:10.3354/ meps202101)
- 19. Ryu S, Pepper RE, Nagai M, France DC. 2016 Vorticella: a protozoan for bio-inspired engineering. Micromachines 8, 4. (doi:10.3390/ mi8010004)
- 20. Hartmann C, Ozmutlu O, Petermeier H, Fried J, Delgado A. 2007 Analysis of the flow field induced by the sessile peritrichous ciliate Opercularia asymmetrica. J. Biomech. 40, 137-148. (doi:10.1016/j.jbiomech. 2005.11.006)
- 21. Kanso EA, Lopes RM, Strickler JR, Dabiri JO, Costello JH. 2021 Teamwork in the viscous oceanic

- microscale. Proc. Natl Acad. Sci. USA 118, e2018193118. (doi:10.1073/pnas.2018193118)
- 22. Canter HM, Walsby AE, Kinsman R, Ibelings BW. 1992 The effect of attached vorticellids on the buoyancy of the colonial cyanobacterium Anabaena lemmermannii. Br. Phycol. J. 27, 65-74. (doi:10. 1080/00071619200650081)
- 23. Subramanian G, Koch DL. 2006 Centrifugal forces alter streamline topology and greatly enhance the rate of heat and mass transfer from neutrally buoyant partides to a shear flow. Phys. Rev. Lett. 96, 134503. (doi:10.1103/PhysRevLett.96.134503)
- 24. Krishnamurthy D, Subramanian G. 2018 Heat or mass transport from drops in shearing flows. Part 1. The open-streamline regime. J. Fluid Mech. 850, 439-483. (doi:10.1017/jfm.2018.439)
- 25. Shanks AL, Trent JD. 1980 Marine snow: sinking rates and potential role in vertical flux. Deep Sea Res. A 27, 137-143. (doi:10.1016/0198-0149(80)90092-8)
- 26. Hawley N. 1982 Settling velocity distribution of natural aggregates. J. Geophys. Res. 87(C12), 9489. (doi:10.1029/JC087iC12p09489)
- 27. Ploug H, Jørgensen BB. 1999 A net-jet flow system for mass transfer and migrosensor studies of sinking aggregates. Mar. Ecol. Prog. Ser. 176, 279-290. (doi:10.3354/meps176279)
- 28. Krishnamurthy D, Li H, Benoit du Rey F, Cambournac P, Larson AG, Li E, Prakash M. 2020 Scale-free vertical tracking microscopy. Nat. Methods 17, 1040-1051. (doi:10.1038/s41592-020-0924-7)
- 29. Cronenberg CCH, Van den Heuvel JC. 1991. Determination of glucose diffusion coefficients in biofilms with micro-electrodes. Biosens. Bioelectron. 6, 255-262. (doi:10.1016/0956-5663(91)80011-L)
- 30. Vacchiano EJ, Kut JL, Wyatt ML, Buhse HE. 1991 A novel method for mass-culturing Vorticella. J. Protozool. 38, 609-613.
- 31. Thielidke W, Stamhuis E. 2014 PIVlab towards user-friendly, affordable and accurate digital particle

- Pepper RE, Krishnamurthy D, Prakash M. 2022
 Data from: Active sinking particles: flow and transport dynamics due to sessile suspension feeders on sinking aggregates. Dryad Dataset.

 Available from: https://doi.org/10.5061/dryad.j6q573nf8.
- Krishnamurthy D, Prakash M, Pepper RE. 2021 Code for: Active sinking particles: flow and transport dynamics due to sessile suspension feeders on sinking aggregates. GitHub. Available from: https:// github.com/deepakkrishnamurthy/active-sinkingparticles.git.
- Schneider CA, Rasband WS, Eliceiri KW. 2012 NIH Image to Image!: 25 years of image analysis. Nat. Methods 9, 671–675. (doi:10.1038/nmeth.2089)
- Gilpin W, Prakash VN, Prakash M. 2017 Flowtrace: simple visualization of coherent structures in biological fluid flows. J. Exp. Biol. 220, 3411–3418.
- Kiørboe T, Jadsson GA. 2001. Marine snow, organic solute plumes, and optimal chemosensory behavior of bacteria. Limnol. Oceanogr. 46, 1309–1318.
- ladson GA, Kiørboe T. 2004 Zooplankton use of chemodetection to find and eat partides. Mar. Ecol. Prog. Ser. 269, 153–162. (doi:10.3354/ meps/69153)
- Lombard F, Koski M, Kiørboe T. 2013 Copepods use chemical trails to find sinking marine snow aggregates. Limnol. Oceanogr. 58, 185–192. (doi:10.4319/lo.2013.58.1.0185)
- Pepper RE, Roper M, Ryu S, Matsumoto N, Nagai M, Stone HA. 2013 A new angle on microscopic suspension feeders near boundaries. Biophys. J. 105, 1796–1804. (doi:10.1016/j.bpj.2013.08.029)

Downloaded from https://royalsocietypublishing.org/ on 08 February 2023

- Rode M, Meucai G, Seegert K, Kiørboe T, Andersen A. 2020 Effects of surface proximity and force orientation on the feeding flows of microorganisms on solid surfaces. Phys. Rev. Fluids 5, 123104. (doi:10.1103/PhysRevFluids.5.123104)
- Berg HC. 1993 Random walks in biology, Revised edn. Princeton, NJ: Princeton University Press.
- Batchelor GK. 2000 An introduction to fluid dynamics.
 Cambridge, UK: Cambridge University Press.

- Pepper RE, Riley EE, Baron M, Hurot T, Nielsen LT, Koehl MAR, Kiørboe T, Andersen A. 2021 The effect of external flow on the feeding currents of sessile microorganisms. J. R. Soc. Interface 18, 20200953. (doi:10.1098/rsif.2020.0953)
- 44. Alldredge AL, Gotschalk C. 1988 In situ settling behavior of marine snow. Limnol. Oceanogr. 33, 339–351. (doi:10.4319/lo.1988.33.3.0339)
- Roper M, Dayel MJ, Pepper RE, Koehl MAR 2013
 Cooperatively generated stresslet flows supply fresh fluid to multicellular choanoflagellate colonies.
 Phys. Rev. Lett. 110, 228104. (doi:10.1103/PhysRevLett.110.228104)
- Suzuki-Tellier S, Andersen A, Kiørboe T. 2022
 Mechanisms and fluid dynamics of foraging in heterotrophic nanoflagellates. Limnol. Oceanogr. 67, 1287–1298. (doi:10.1002/no.12077)
- Hemdl GJ. 1988 Ecology of amorphous aggregations (marine snow) in the northern Adriatic Sea. 2.
 Microbial density and activity in marine snow and its implication to overall pelagic processes. Mar. Ecol. Prog. Ser. 48, 265–275. (doi:10.3354/meps048265)
- Liron N, Blake JR. 1981 Existence of viscous eddies near boundaries. J. Fluid Mech. 107, 109–129. (doi:10.1017/S0022112081001699)
- Leal LG. 2007 Advanced transport phenomena: fluid mechanics and convective transport processes, vol. 7.
 Cambridge, UK: Cambridge University Press.
- Karp-Boss L, Boss E, Jumars PA. 1996 Nutrient fluxes to planktonic osmotrophs in the presence of fluid motion. Oceanogr: Mar. Biol. Annu. Rev. 34, 71–107.
- Acrivos A. 1971 Heat transfer at high Pédet number from a small sphere freely rotating in a simple shear field. J. Fluid Mech. 46, 233–240. (doi:10. 1017/S0022112071000508)
- Batchelor GK. 1980 Mæs transfer from small partides suspended in turbulent fluid. J. Fluid. Med. 98, 609–623. (doi:10.1017/ S002211208000304)
- Magar V. 2003 Nutrient uptake by a self-propelled steady squirmer. Q. J. Meth. Appl. Math. 56, 65–91. (doi:10.1093/qjmam/56.1.65)
- Kanso EA, Lopes RM, Strickler JR, Dabiri JO, Costello JH. 2021 Teamwork in the viscous oceanic

- microscale. Proc. Natl Acad. Sci. USA 118, e2018193118. (doi:10.1073/pnas.2018193118)
- Jackson GA 2001 Effect of coagulation on a model planktonic food web. Deep Sea Res. Part I 48, 95–123. (doi:10.1016/S0967-0637(00)00040-6)
- Jackson GA, Burd AB. 2015 Simulating aggregate dynamics in ocean biogeochemical models. Prog. Oceanogr. 133, 55–65. (doi:10.1016/j.pocean.2014. 08.014)
- Li X, Logan BE. 1997 Collision frequencies of fractal aggregates with small particles by differential sedimentation. Environ. Sci. Technol. 31, 1229–1236. (doi:10.1021/es960771w)
- Li XY, Yuan Y. 2002 Collision frequencies of microbial aggregates with small particles by differential sedimentation. Environ. Sci. Technol. 36, 387–393. (doi:10.1021/es010681d)
- Christensen-Dalsgaard KK, Fenchel T. 2003 Increased filtration efficiency of attached compared to freeswimming flagellates. Aquat. Microb. Ecol. 33, 77–86. (doi:10.3354/ame033077)
- Andersen A, Kiørboe T. 2020 The effect of tethering on the dearance rate of suspension-feeding plankton. Proc. Natl Acad. Sci. USA 117, 30101–30103. (doi:10.1073/pnas.2017441117)
- Menden-Deuer S, Kiørboe T. 2016 Small bugs with a big impact: linking plankton ecology with ecosystem processes. J. Plankton Res. 38, 1036–1043. (doi:10.1093/plankt/fbw049)
- Litchman E, Chman MD, Kiørboe T. 2013 Trait-based approaches to zooplankton communities. J. Plankton Res. 35, 473–484. (doi:10.1093/plankt/fbt019)
- Kiørboe T. 2008 A mechanistic approach to plankton ecology, illustrated edn. Princeton, NJ: Princeton University Press.
- Koehl MAR. 2007 Mini review: hydrodynamics of larval settlement into fouling communities.
 Biofouling 23, 357–368. (doi:10.1080/ 08927010701492250)
- Krishnamurthy D, Pepper R, Prakash M. 2023 Active sinking particles: sessile suspension feeders significantly alter the flow and transport to sinking aggregates. Figshare. (doi:10.6084/m9.figshare.c. 6384910)